JURNAL KIMIA VALENSI
p-ISSN: 2460-6065; e-ISSN: 2548-3013
Journal homepage: https://journal.uinjkt.ac.id/index.php/valensi
Research Article

Potential Antidiabetic Activity of *Annona muricata* Leaves as Enzyme α-amylase Inhibitor: *In Silico* Study

Zahra Putri Handirana [1], Tresna Lestari [1], Richa Mardianingrum[2], Ruswanto Ruswanto[1*]

[1]*Department of Medicinal Chemistry, Faculty of Pharmacy, Universitas Bakti Tunas Husada, Jl. Cilolohan No. 36, Tasikmalaya, 46115, Indonesia*
[2]*Department of Pharmacy, Faculty of Health Science, Universitas Perjuangan, Jl. PETA No. 177, Tasikmalaya, 46115, Indonesia*

[*]*Email: ruswanto@universitas-bth.ac.id*

Article Info
Received: Apr 24, 2025
Revised: May 17, 2026
Accepted: May 25, 2026
Online: June 6, 2026

Citation:
Handirana, Z. H., Lestari , T., Mardianingrum, R., Ruswanto, R. (2026). Potential Antidiabetic Activity of *Annona muricata* Leaves as Enzyme α-amylase Inhibitor: *In Silico* Study *Jurnal Kimia Valensi*, 12(1), 132-143.

Doi: 10.15408/jkv.v12i1.46091

Abstract

Diabetes mellitus is a prevalent metabolic disorder requiring effective and safe therapeutic approaches. Natural compounds have gained attention as potential alternatives to synthetic drugs such as acarbose, which may cause adverse effects. This study aimed to evaluate the antidiabetic potential of secondary metabolites from Annona muricata leaves as α-amylase inhibitors using an in-silico approach. Molecular docking (PyRx), molecular dynamics simulation (Desmond, 100 ns), and ADMET prediction were performed to assess binding affinity, stability, and drug-likeness properties. Among the tested compounds, three lead compounds exhibited the strongest binding affinity: coclaurine (-9.25 kcal/mol), (+)(-) Xylopine (-8.94 kcal/mol), and annomuricine (-8.82 kcal/mol) compared to acarbose (-4.95 kcal/mol). Molecular dynamics analysis demonstrated annomuricine was the most stable interaction with key catalytic residues (Asp197, Glu233, and Asp300). Additionally,annomuricine satisfied Lipinski's Rule of Five and showed favorable pharmacokinetic profiles, although it interacted with CYP enzymes. In conclusion, annomuricine demonstrates strong potential as a natural α-amylase inhibitor and may serve as a promising candidate for antidiabetic drug development. However, further in vitro and in vivo studies are required to validate these findings.

Keywords: Acarbose, *Annona muricata*, antidiabetic, α-amylase

1. INTRODUCTION

Diabetes mellitus (DM) remains a major global health problem characterized by chronic hyperglycemia and severe long-term complications that negatively affect patients' quality of life. According to the World Health Organization (WHO), diabetes causes approximately 1.5 million deaths annually worldwide, reflecting its significant global burden [1]. The increasing prevalence of diabetes highlights the urgent need for effective, safe, and affordable therapeutic strategies. Early diagnosis and proper treatment are important to prevent complications, reduce premature mortality, and improve patient quality of life [2].

Diabetes mellitus is a chronic metabolic disorder caused by impaired insulin secretion, insulin action, or both, leading to persistent hyperglycemia [3]. The disease develops through complex interactions between genetic and environmental factors [4]. Type 1 diabetes is characterized by autoimmune destruction of pancreatic β-cells, whereas type 2 diabetes is associated with obesity, insulin resistance, and impaired insulin secretion. Current diabetes management focuses on glycemic control using oral and injectable antihyperglycemic agents [5]. One important therapeutic target is the α-amylase enzyme, which plays a major role in carbohydrate digestion and glucose absorption. Inhibition of α-amylase can reduce postprandial blood glucose levels, making this enzyme an important target in antidiabetic therapy [6].

Acarbose is a clinically used α-amylase and α-glucosidase inhibitor; however, its long-term use is

often associated with gastrointestinal side effects and impaired liver function [7,8]. Therefore, there is growing interest in discovering natural compounds with antidiabetic activity that possess fewer side effects and lower treatment costs [9]. One promising medicinal plant is soursop (*Annona muricata L.),* which contains various bioactive secondary metabolites such as alkaloids, flavonoids, phenolics, acetogenins, steroids, and saponins. Pharmacological studies have demonstrated that *Annona muricata* exhibits anticancer, antioxidant, antimicrobial, anti-inflammatory, and antihyperglycemic activities [10–12]. In diabetes management, soursop leaves are known to inhibit α-amylase and α-glucosidase, thereby reducing postprandial glucose levels [13].

Several metabolites from *Annona muricata*, particularly coclaurine and xylopine, are believed to contribute to α-amylase inhibition through interactions with the enzyme's active site. Experimental studies support these findings. Kusuma (2021) reported that the ethanol extract of soursop leaves significantly reduced blood glucose levels in glucose-induced mice [14], while Opara (2021) demonstrated similar antihyperglycemic effects in alloxan-induced Wistar rats [15]. Despite these findings, molecular-level studies evaluating the interaction of individual metabolites with α-amylase remain limited. Therefore, this study aims to conduct a comprehensive in silico investigation using molecular docking, molecular dynamics simulation, and ADMET analysis to identify potential antidiabetic compounds from *Annona muricata* leaves.

2. RESEARCH METHODS

The α-amylase enzyme (PDB ID: 3BLP) was selected as the target receptor because of its important role in carbohydrate metabolism and its relevance as a therapeutic target for diabetes mellitus [16]. The crystal structure with a resolution of 1.60 Å was retrieved from the Protein Data Bank (https://www.rcsb.org). Receptor validation was performed using Ramachandran plot analysis, ERRAT, and VERIFY3D to confirm structural and stereochemical quality. Receptor preparation included removal of water molecules and native conformers, followed by native ligand separation using Molegro Molecular Viewer [17]. Hydrogen atoms and partial charges were added using BIOVIA Discovery Studio 2021 [18]. Docking validation in PyRx 0.9.8 used 150 GA runs and was considered valid when RMSD was <2 Å.

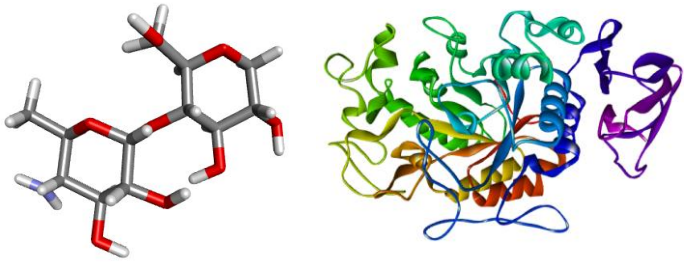

(a) (b)

Figure 1. The 3D structure of the natural ligand (a) and the protein (b)

Ligand Preparation

A total of 203 secondary metabolites contained in soursop leaves were obtained from the https://www.knapsackfamily.com/jamu/top.php website then downloaded from the https://pubchem.ncbi.nlm.nih.gov/ website and downloaded in 2D format .sdf and converted into .mol2 format. Using MarvinSketch software, each compound was cleaned in 2D format and then protonated at pH 7.4 according to the pH of blood and stored in .mrv format. Furthermore, energy minimization was carried out using the *Merck Molecular Force Field* (MMFF94) conformation with a total of 10 conformations, then stored in .pdb format. MMFF94 is a type of energy minimization equation used in organic compounds [19].

Molecular Docking

Virtual screening of ligand compounds that have been prepared was carried out on *PyRx* Virtual Screening Tool 0.9.8 software with the Autodock Wizard method. The docking process was carried out on 203 compounds in .pdbqt format with macromolecules in the form of receptors that had been prepared and validated to see their interactions with potential targets. This process uses a gridbox that has been validated previously by running 150 GA runs for 150 times. The binding affinity value between each ligand and the receptor was obtained, and the three best compounds with the lowest binding value were selected. The three compounds that have the lowest

value were coclaurine, (+)-(+)(-) Xylopine, and annomuricine.

Molecular Dynamics

The selected compounds, along with the native ligand and the standard drug acarbose, were further analyzed through a 100 ns molecular dynamics (MD) simulation using the academic version of Desmond Release 2019 (Schrödinger, LLC, New York, NY, USA). The simulation conditions included the TIP3P water model, 0.15 M NaCl concentration, and an NPT ensemble maintained at 300 K and 1.01325 bar within an orthorhombic simulation box measuring 10 Å × 10 Å × 10 Å [20].

Drug Scan, Pharmacokinetic and Toxicity Profile Prediction

Drug-likeness evaluation was conducted according to Lipinski's Rule of Five using the SCFBio platform. In addition, pharmacokinetic and toxicity characteristics were assessed using the pkCSM server to predict ADMET properties, including absorption, distribution, metabolism, excretion, and toxicity [18,21].

3. RESULTS AND DISCUSSION

The Receptor Identification Results

Prior to molecular docking analysis, receptor validation was an essential step to ensure that the selected protein structure possesses good stereochemical quality and structural stability. Validation of the receptor structure was important because the accuracy of ligand–receptor interaction studies was strongly influenced by the quality of the protein model used. In this study, the α-amylase enzyme with PDB code 3BLP was evaluated using Ramachandran plot analysis and quality factor assessment to determine the reliability and suitability of the receptor for molecular docking simulations. The results of these validation analyses are presented in **Figures 2** and **Figure S1**.

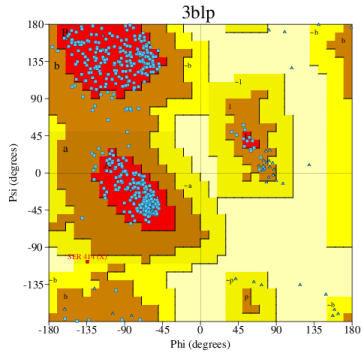

PROCHECK statistics

1. Ramachandran Plot statistics

		No. of residues	%-tage
Most favoured regions	[A,B,L]	378	90.0%*
Additional allowed regions	[a,b,l,p]	41	9.8%
Generously allowed regions	[~a,~b,~l,~p]	1	0.2%
Disallowed regions	[XX]	0	0.0%
Non-glycine and non-proline residues		420	100.0%
End-residues (excl. Gly and Pro)		2	
Glycine residues		51	
Proline residues		22	
Total number of residues		495	

Figure 2. The Ramachandran plot of enzyme *α-amylase* (3BLP.pdb)

The Ramachandran plot (**Figure 2**) analysis of the α-amylase receptor (3BLP.pdb) demonstrated that the protein structure possessed good stereochemical quality and was suitable for molecular docking studies. The PROCHECK statistics showed that 90.0% of amino acid residues were located in the most favored regions, indicating that the majority of the backbone dihedral angles (φ and ψ) adopted energetically favorable conformations [22]. In addition, 9.8% of residues were found in the additionally allowed regions, while only 0.2% were present in the generously allowed regions. Importantly, no residues were detected in the disallowed regions, suggesting the absence of significant structural distortions or unfavorable conformations within the protein structure.

A high percentage of residues in the most favored regions reflects the structural stability and reliability of the receptor model. Generally, a protein structure is considered valid and of good quality when more than 90% of residues are distributed within the favored regions of the Ramachandran plot. The absence of residues in disallowed regions further confirms that the α-amylase receptor has an acceptable geometric configuration and appropriate torsional angles for protein modeling studies [23]. Therefore, the 3BLP receptor structure can be considered accurate and reliable for subsequent molecular docking and molecular dynamics simulations in evaluating ligand–receptor interactions [24,25]. The absence of residues in the *disallowed* region means that are no deviations that occur in the protein structure used [26,27].

Profile checking, ERRAT analysis, and 3D VERIFY were performed on the web https://saves.mbi.ucla.edu, which is able to predict various types of stereochemical parameters of protein structures [22].

The overall quality factor value in the ERRAT analysis shown in **Figure S1** was 96.091%. An ERRAT value of 95% or higher indicates a good high-resolution model. This means that the atomic environment is in the acceptable region[28]. No error

peaks were detected at positions 140-160 and 220-240, which means no potential errors were found. Based on the analysis, the structure of enzyme *α-Amylase* with PDB code 3BLP has a high-resolution structure and can be used in ligand-receptor interaction studies[29].

The Docking Validation Results

The previously separated receptor was validated by re-docking the *α-amylase* enzyme receptor with the natural ligand (GLC-AGL) for 150 conformations using the *Genetic algorithm (GA)* with a 0.375 Å spacing setting in the PyRx application.

Validation of the docking method yielded an RMSD of 0.62 Å. RMSD (*Root Mean Square Deviation*) value is a value that shows the distance between the bond position of the natural ligand with protein after *re-docking* and the actual bond position. This RMSD value is used as a validation parameter[30]. An RMSD value <2Å indicates that the method is valid [20]. In addition to the RMSD value, the lowest binding value obtained was -3.83 kcal/mol; this value indicates that the interaction of ligand and receptor is quite stable. Gridbox setting as one of the docking parameters was set with grid center coordinate X = 2.692, Y = 40.975, and Z = 24.196, with a *grid box* size of 40 Å each. This setting was made so that the active site of the receptor can be reached as much as possible (**Table S1**).

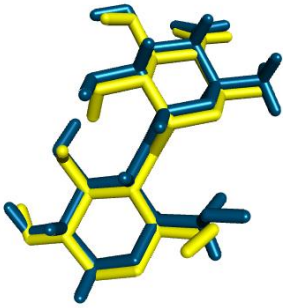

Figure 3. Structure of natural ligand GLC-AGL of crystallography (Blue) and after *re-docking* process (Yellow)

The binding affinity (kcal/mol) of the ligand complex with the *α-amylase enzyme* receptor was obtained using PyRx with the same parameters during the validation process. *The docking* process was carried out by tethering the receptor with three test compounds (coclaurine, (+)-(+)(-)Xylopine, and annomuricine) as well as a comparator in the form of natural ligands, namely GLC-AGL and antidiabetic drug *acarbose.* Docking process was conducted for 150 conformations and obtained the binding affinity value (kcal/mol) of each compound against the *α-amylase* enzyme receptor.

Table 1. The docking results of compounds against α-amylase enzyme

No.	Compound Name	Binding affinity	Run	Inhibition Constant
1.	*Acarbose*	-4.95	51	234.04
2.	Natural ligands	-4.47	53	531.54
3.	Coclaurine	-9.25	93	166.13
4.	(+)(-) Xylopine	-8.94	89	281.71
5.	Annomuricine	-8.82	138	344.79

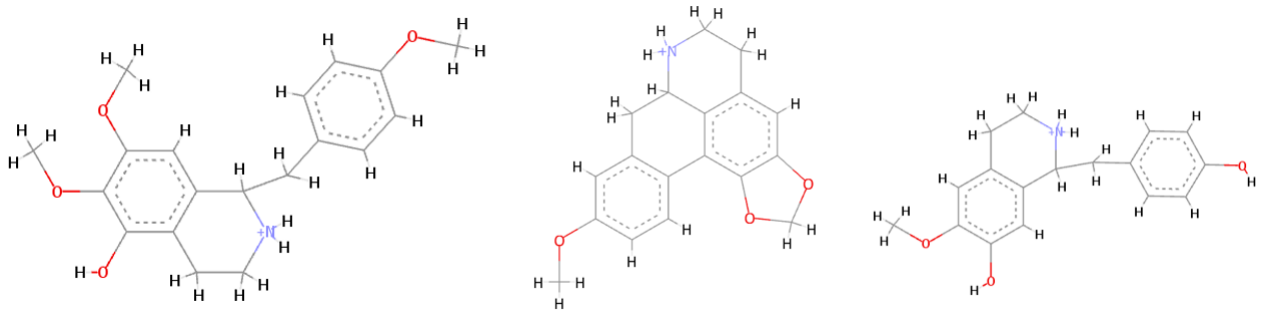

(a) (b) (c)

Figure 4. The 2D structure of annomuricine (a); (+)(-) xylopine (b); coclaurine (c)

The molecular docking analysis of 203 secondary metabolites derived from soursop (*Annona muricata L.*) leaves against the α-amylase receptor identified three compounds with the most favorable binding affinity values. Among them, coclaurine exhibited the strongest interaction, with a binding affinity of −9.25 kcal/mol obtained in the 93rd docking run and an inhibition constant of 166.13 nM. The

second-best interaction was observed for (+)(−) xylopine, which showed a binding affinity value of −8.94 kcal/mol in the 89th run and an inhibition constant of 281.71 nM. Meanwhile, annomuricine demonstrated a binding affinity of −8.82 kcal/mol in the 138th run, accompanied by an inhibition constant of 344.79 nM (**Table 1**).

Acarbose was used as a comparison drug as it shares the same mechanism of action on the *α-amylase* enzyme. The docking results showed that *Acarbose* had a binding affinity of -4.95 kcal/mol, and another natural ligand (GLC-AGL) showed a binding affinity of -4.47 kcal/mol. The binding affinity value is a parameter to assess the ability of the drug to bind to the receptor. The smaller the binding affinity value, the higher the affinity of the receptor and ligand[31,32]. Comparison of docking results between test compounds and comparators showed that metabolite compounds in soursop leaves potentially have stronger binding affinity to *α-amylase* enzyme than natural ligands and *Acarbose*. The ability of a compound to interact with the target receptor was evidenced by its stronger binding affinities (More negative values) compared to the reference compound. This showed that Coclaurine, (+)(-) Xylopine, and Annomuricinewere compounds that had potential as *α-amylase* enzyme inhibitors. The stability of the interaction between the ligand and the receptor is strongly influenced by the binding affinity value. The more negative the value, the smaller the energy used by the test compound to interact with the receptor, so that the interaction can take place stably and spontaneously [33]. The lower binding affinity of coclaurine, (+)(-) xylopine, and annomuricine compared to acarbose suggests a stronger interaction with the α-amylase active site, which may enhance its inhibitory potential,. This indicates that bioactive compound from *Annona muricata* leaves could serve as a promising lead compound for antidiabetic drug development, particularly as a natural alternative with potentially improved efficacy. However, further experimental validation is required to confirm its biological activity. From the docking results, coclaurine exhibited the lowest binding afinity supported by 2D and 3D visualizations of the α-amylase–coclaurine complex to illustrate the interactions between the receptor and ligand, as presented in **Figure 5** (another 2D/3D visualization in **Figure S2**).

The interaction between the α-amylase enzyme and the best docking compounds was visualized to identify important amino acid residues involved in ligand binding at the enzyme's active site. These interactions reflect the molecular contacts formed between the ligand and receptor, where amino acid residues within the binding pocket interact with ligands through hydrophobic, hydrophilic, and hydrogen bonding interactions [34]. Such interactions are essential because they contribute to the stability and affinity of ligand–receptor complexes (can be seen in **Table 2**).

Visualization of acarbose interaction with the α-amylase receptor identified 10 amino acid residues involved in ligand binding. Hydrophilic interactions through hydrogen bonds were observed at His:305, Asp:300, Trp:59, and Gln:63, whereas Gly:306, His:299, Tyr:62, Leu:165, Glu:60, and Trp:58 contributed through hydrophobic interactions. These residues were used as reference points to compare the interaction profiles of coclaurine, (+)(−) xylopine, and annomuricine against the α-amylase receptor.

Coclaurine interacted with 15 amino acid residues and shared five residues with acarbose, including His:305 and Gly:306 through hydrogen bonding, as well as Trp:58, Asp:300, and Trp:59 through hydrophobic interactions. (+)(−) Xylopine also interacted with 15 residues and exhibited six residues similar to acarbose, involving His:305, His:299, Trp:58, Asp:300, Tyr:62, and Gly:306. Annomuricine showed the greatest similarity to acarbose, sharing seven amino acid residues, including His:305, Gly:306, Gln:63, Tyr:62, His:299, Trp:58, and Trp:59.

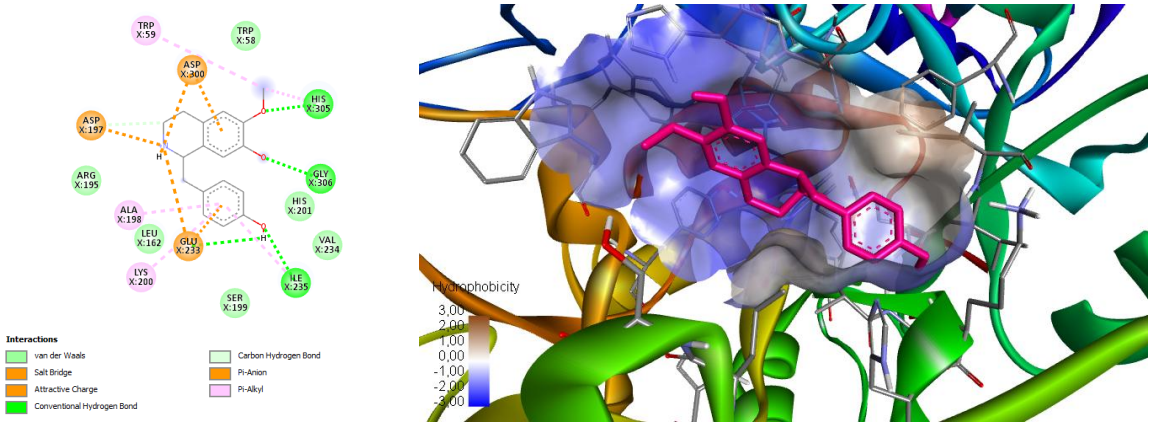

Figure 5. The 2D/3D visualization of *α-amylase* – coclaurine

Table 2. Residues interaction of coclaurine, (+)(-)xylopine, annomuricine, GLC-AGL and *acarbose* on *α-amylase* enzyme

No.	Test Compound	Residue Amount	Residue Type	
			Conventional Hydrogen bonds	Hydrophobic Bonds
1.	Coclaurine	15	3 (**His:305**, **Gly:306**, Ile:235)	12 (**Trp:58**, His:201, Val:234, Ser:199, Arg: 195, Leu: 162, **Asp:300**, Glu:233, Asp:197, **Trp:59**, Ala:198, Lys:200)
2.	(+)(-) Xylopine	15	1 (**His:305**)	14 (**Gly:306**, Val:234, Leu:162, Ala:198, **His:299**, **Trp:58**, **Asp:300**, Asp:197, **Tyr:62**, Glu:233, Lys:200, His:201, Ile:235, Arg:195)
3.	Annomuricine	15	2 (**His:305, Gly:306**)	13 (**Gln:63**, **Tyr:62**, His:101, Arg:195, **His:299, Trp:58**, **Trp:59**, Asp:300, Glu:233, Asp:197, Ala:198, Leu:165, Leu:162)
4.	GLC-AGL (Natural Ligand)	21	4 (**His:299**, Arg:195, Asp:300, Glu:233)	19 (**Tyr:62**, Asp:197, Ile:235, His:201, Lys:200, Val:234, Ser:199, **Gly:306**, Ala:198, Leu:162, **Leu:165**, Tyr:151, His:305, Ser:163, Trp:59, **Trp:58**, His: 101)
5.	*Acarbose*	10	**4 (His:305, Asp:300, Trp:59, Gln:63)**	**6 (Gly:306, His:299, Tyr:62, Leu:165, Glu:60, Trp:58)**

The α-amylase active site contains three essential catalytic residues, namely Asp197, Glu233, and Asp300, which are crucial for starch hydrolysis. Molecular dynamics simulations demonstrated that the tested compounds interacted with these residues, indicating their ability to bind at the active site [35]. Asp197 functions as a catalytic nucleophile, Glu233 acts as an acid–base catalyst, and Asp300 stabilizes substrate orientation during catalysis.

Hydrophilic and hydrophobic interactions collectively contribute to ligand–receptor stability [36,37]. Hydrogen bonding strengthens electrostatic interactions, whereas hydrophobic contacts stabilize nonpolar interactions and reduce water interference, thereby enhancing ligand binding affinity [38]. Among the tested, three compound from annona muricata leaf exhibited stable interactions with Asp197, Glu233, and Asp300, suggesting strong inhibitory potential against α-amylase through active-site binding and interference with carbohydrate hydrolysis.

Molecular Dynamics Simulation Analysis

The ability to maintain the stability of the docking result compounds was evaluated by using Desmond program version 2019 free academic[39]. This process was carried out to see the stability of each test compound that interacted with the α-amylase receptor, which was then compared after going through the molecular dynamics process for 100ns. The stability of each compound can be seen from the RMSD graphs (**Figures 6** and **7**).

Figure 6 illustrates the RMSD changes over time as a parameter to evaluate the stability of ligand–receptor complexes during molecular dynamics simulation. Lower and more stable RMSD values indicate greater conformational stability and stronger inhibitory potential of the compounds toward the α-amylase enzyme. Coclaurine, (+)(−) xylopine, and annomuricine were represented by gray, yellow, and blue lines, respectively. All three compounds exhibited RMSD values within the range of 1–2.2 Å and maintained relatively stable profiles with only slight fluctuations. Minor fluctuations occurred in the 17.4–40.6 ns region for coclaurine and (+)(−) xylopine, and in the 43.5–58.0 ns region for annomuricine. These findings indicate that all three compounds were able to interact stably with the α-amylase receptor and therefore possess potential as α-amylase inhibitors for diabetes mellitus treatment. Among them, annomuricine demonstrated the most stable RMSD profile with the lowest fluctuations (detailed RMSD average in **Table S2**).

In comparison, the native ligand GLC-AGL and the reference drug acarbose showed higher RMSD fluctuations reaching up to 2.8 Å. According to Mardianingrum in Prasetiawati et al., higher fluctuations indicate unstable interactions due to significant positional changes during molecular dynamics simulations [41]. The lower fluctuation values observed in the soursop-derived compounds suggest that these metabolites formed more stable and active interactions at the binding site than GLC-AGL and acarbose. Consequently, these compounds may have greater potential for development as antidiabetic agents.

RMSF analysis (Figure 7) was conducted to evaluate residue flexibility and fluctuations in amino acid residues during ligand interaction [42]. Significant

fluctuations were observed in residue regions 98, 140, 308, 350, and 462, with the highest fluctuation occurring around residue 350, particularly in the acarbose complex. Table S3 presents the lowest and highest RMSF values of each compound and their associated residues. Lower RMSF values indicate stronger and more stable interactions, whereas higher RMSF values suggest weaker and less stable binding [43] (detailed RMSF average in **Table S3**). Coclaurine, xylopine, and annomuricine showed the lowest RMSF values of 0.345 Å, 0.345 Å, and 0.382 Å, respectively, all involving the Arg195 residue. These values were lower than those of GLC-AGL (0.443 Å at Asn46) and acarbose (0.412 Å at Met338). The highest RMSF values were observed at residues Asn350 for coclaurine and xylopine (4.541 Å) and Asn364 for annomuricine (4.055 Å), whereas acarbose exhibited the highest fluctuation at Gly351 (7.021 Å).

Secondary structure element (SSE) analysis during the 100 ns simulation was performed to evaluate changes in the protein's 3D structure [44]. The annomuricine–α-amylase complex showed that 36.45% of protein residues were maintained in secondary structures, consisting of 16.94% α-helix and 19.51% β-strand conformations (**Figure S3**).

The interaction between annomuricine and the α-amylase receptor was monitored throughout the 100 ns molecular dynamics simulation. **Figure 8** demonstrates the various amino acid residues involved in ligand–protein interactions during the simulation period. Several interaction types were observed, including hydrogen bonds, hydrophobic interactions, ionic bonds, and water bridges, all of which contributed to ligand–receptor stability. Among these interactions, hydrogen bonds were the most dominant and are known to enhance stability while promoting biological responses at the target protein [45]. Key hydrogen bond interactions involved residues Asp197, Gln663, Asp300, His305, and Gly3066. Notably, Asp197and Asp300 maintained strong hydrogen bond interactions for nearly 100% of the simulation time. Since Asp197, Glu233, and Asp300 are essential catalytic residues located at the active site of α-amylase, these interactions strongly support the binding potential of annomuricine toward the enzyme's active site.

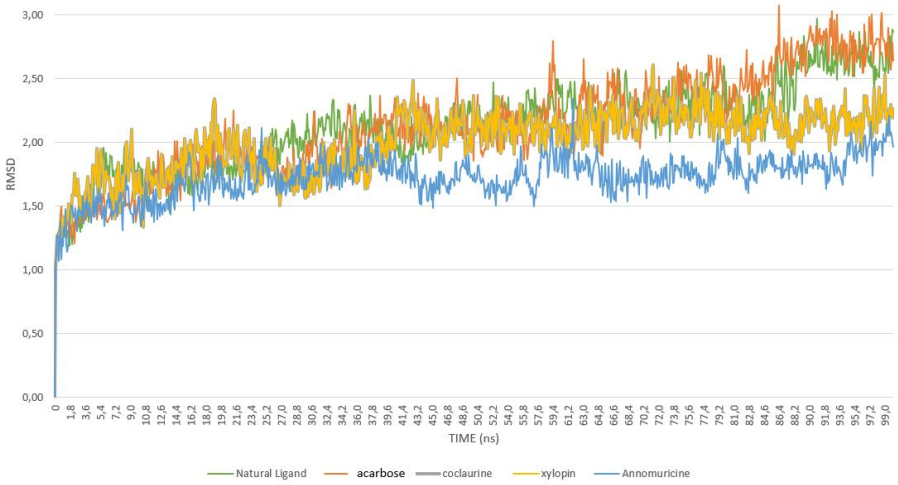

Figure 6. The RMSD of the ligand-receptor complex in molecular dynamics for 100ns

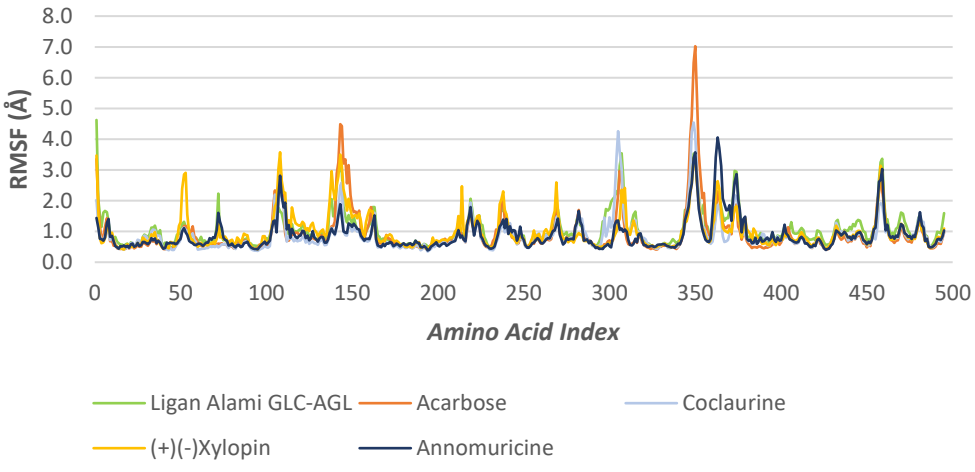

Figure 7. The RMSF of the ligand-receptor complex at 100ns

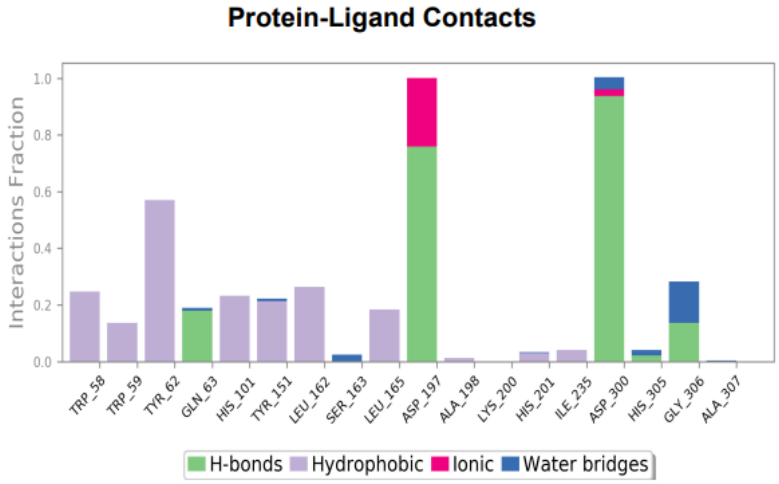

Figure 8. Protein ligand contact of annomuricine and enzyme α-amylase in molecular dynamics 100ns.

Table 3. Lipinski's profile of test compounds

Compound	Number of H-bond Donors (<5)	Number of H-bonded acceptors (<10)	Molecular Weight (<500)	LogP (0-5)	Molar Refractivity (40-130)
Annomuricine	1	4	329	3.15523	90.503288
Coclaurine	2	3	285	2.26445	79.006909
(+)(-) Xylopine	1	3	295	1.94557	79.120193

Table 4. Pharmacokinetic profile of test compounds

Parameters		Coclaurine	(+)(-) Xylopine	Annomuricine	Unit
Property	**Model name**		**Value**		
Absorption	Water solubility	-3.27	-2.972	-3.077	(log mol/L)
Absorption	$Caco_2$ permeability	1.165	1.647	1.221	(log P in 10^{-6} cm/s)
Absorption	Intestinal absorption (human)	92.875	91.985	90.876	(% Absorbed)
Distribution	VDss (human)	-2.782	1.027	0.996	(log L/kg)
Distribution	BBB permeability	0.177	0.343	-0.332	(log BB)
Metabolism	CYP2D6 substrate	Yes	No.	Yes	(Yes/No)
Metabolism	CYP1A2 inhibitor	Yes	Yes	Yes	(Yes/No)
Excretion	Total Clearance	1.075	1.073	1.003	(log ml/min/kg)
Excretion	Renal OCT2 substrate	No.	No.	No.	(Yes/No)
Toxicity	AMES toxicity	No.	Yes	No.	(Yes/No)
Toxicity	Oral Rat Acute Toxicity (LD50)	2.713	3.531	2.902	(mol/kg)"

Hydrophobic interactions also contributed significantly to complex stability, particularly through residues Trp58, Trp59, Tyr62, His101, Tyr151, Leu162, Leu165, His201, and Ile235. Tyr62 maintained hydrophobic interactions for approximately 50% of the simulation duration. In addition, water bridge interactions were strongly observed at residues Gly306 and Ser163 through water-mediated contacts [46]. Some amino acids formed multiple interaction types simultaneously, such as Asp197, which participated in both ionic and hydrogen bonding, and Asp300, which formed hydrogen bonds, ionic interactions, and water bridges.

Figure S4 shows that the total number of ligand–protein contacts remained relatively stable throughout the simulation with only minor fluctuations, indicating consistent interaction stability. Residues Asp197 and Asp300 exhibited the most intense and persistent contacts, highlighting their critical role in stabilizing the complex.

The ligand torsion profile shown in **Figure S5** further demonstrated that most rotatable bonds within the annomuricine structure maintained stable conformations during the simulation. Dense clustering of torsion angles and narrow histogram distributions indicated limited conformational fluctuations, supporting the presence of an optimal conformation

for strong and selective binding to the active site of α-amylase.

Drug Scan and ADMET Prediction

A compound can be considered drug-like if the compound meets a series of parameters in Lipinski's Rule of Five (RO5). These parameters are used to assess problems in bioavailability. If a compound violates at least two RO5 criteria then bioavailability problems may occur. Ideally, a compound has good permeability if it has the number of hydrogen bond donors less than 5 and the number of hydrogen bond acceptors less than 10, molecular weight less than 500 g/mol, Log P less than 4.5 and molar refractivity in the range of 40-130 [47,48].

Table 3 presents the physicochemical and pharmacokinetic analysis of the tested compounds. The results demonstrated that all three compounds fulfilled the criteria of Lipinski's Rule of Five (RO5), indicating favorable drug-likeness properties. The number of hydrogen bond donors and acceptors in each compound met the accepted criteria, suggesting that the absorption process requires relatively low energy and can occur efficiently [49]. In addition, the molecular weights of the compounds ranged from 250–350 Daltons, which is within the Lipinski requirement of less than 500 Daltons. Compounds with lower molecular weight generally exhibit improved diffusion through cell membranes, leading to enhanced absorption and permeability in the digestive tract [50].

The LogP values of all compounds were below 5, indicating favorable lipophilicity and the ability to penetrate the lipid bilayer of cell membranes. Compounds with LogP values greater than 5 are generally more difficult to absorb, less capable of interacting with target proteins, and may exhibit toxic effects because of strong membrane binding [50–52]. Furthermore, all compounds met the acceptable molar refractivity criteria, suggesting good molecular polarizability, which is an important parameter in drug–receptor interactions [53]. Overall, the compounds isolated from soursop leaves fulfilled the requirements of Lipinski's RO5, supporting their potential as orally active drug candidates.

Pharmacokinetic screening (**Table 4**) included absorption, distribution, metabolism, excretion, and toxicity (ADMET) parameters. Absorption analysis involved water solubility, Caco-2 permeability, and intestinal absorption. Among the tested compounds, (+)(−) xylopine demonstrated the best water solubility with a value of −2.972 log mol/L and showed the highest permeability through Caco-2 cells with a permeability value of 1.647. All compounds exhibited high intestinal absorption values exceeding 90%, with coclaurine showing the highest absorption percentage at 92.875%.

In the distribution profile, (+)(−) xylopine exhibited the highest VDss value at 1.027 log L/kg, indicating greater distribution into plasma and tissue compartments [48]. Blood–brain barrier (BBB) permeability is considered favorable when the value exceeds 0.3, although some studies report that BBB penetration occurs at values above 1 [50,54]. The tested compounds generally showed low BBB permeability. However, this characteristic is not considered problematic because α-amylase inhibitors primarily act in the digestive tract to delay starch breakdown and regulate postprandial blood glucose levels, rather than targeting the central nervous system.

Metabolic analysis evaluated whether the compounds acted as CYP2D6 substrates and CYP1A2 inhibitors, both of which are important cytochrome P450 enzymes involved in hepatic drug metabolism. Coclaurine and annomuricine were identified as CYP2D6 substrates and CYP1A2 inhibitors, whereas (+)(−) xylopine was not a CYP2D6 substrate but still inhibited CYP1A2. These findings suggest that coclaurine and annomuricine may undergo hepatic metabolism, while all compounds could potentially influence the metabolism of co-administered drugs [55].

Excretion analysis showed that coclaurine had the highest total clearance value (1.075 log ml/min/kg), indicating the fastest elimination rate, whereas annomuricine exhibited the slowest elimination profile (1.003 log ml/min/kg) [56,57]. None of the compounds were substrates of renal OCT2, suggesting a low risk of adverse interactions with OCT2 inhibitors. Toxicity prediction revealed that only (+)(−) xylopine showed mutagenic potential based on Ames toxicity analysis. In contrast, coclaurine and annomuricine were predicted to be non-mutagenic. Coclaurine exhibited the lowest acute toxicity, while (+)(−) xylopine demonstrated the highest predicted acute toxicity with an LD50 value of 3.531 mol/kg.

4. CONCLUSIONS

This study provides a comprehensive in silico evaluation of secondary metabolites from *Annona muricata* leaves as potential α-amylase inhibitors, highlighting annomuricine as the most promising candidate. Compared to acarbose, annomuricine demonstrated stronger binding affinity, stable interactions with key catalytic residues (Asp197, Glu233, and Asp300), and favorable drug-likeness properties, suggesting its potential role in inhibiting α-amylase activity at the molecular level.

Importantly, this study represents one of the first comprehensive in silico reports systematically evaluating *Annona muricata* leaf metabolites against α-amylase in comparison with a standard drug. These findings contribute to the identification of natural

compounds as potential lead candidates for antidiabetic drug development.

However, it should be emphasized that the present results are preliminary and based solely on computational approaches. Therefore, further experimental validation through in vitro and in vivo studies is required to confirm the inhibitory activity, safety, and therapeutic potential of annomuricine as a natural antidiabetic agent.

ACKNOWLEDGMENTS

The authors would like to thank all collaborators from Universitas Bakti Tunas Husada and Universitas Perjuangan Tasikmalaya.

REFERENCES

1. World Health Organization. Diabetes. Published 2023. Accessed April 16, 2024. https://www.who.int/health-topics/diabetes#tab=tab_1
2. International Diabetes Federation. *IDF Diabetes Atlas*. 10th ed. (Boyko EJ, Magliano DJ, Karuranga S, Piemonte L, Saeedi PRP, Sun H, eds.); 2021.
3. Sani FN, Widiastuti A, Ulkhasanah ME, Amin NA. Overview of Quality of Life in Diabetes Mellitus Patients. *J Nurse Research Prof*. 2023;5(3):1151-1158. https://ejournal.helvetia.ac.id/jdg%0Ahttp://jurnal.globalhealthsciencegroup.com/index.php/JPPP
4. Budianto RE, Linawati NM, Arijana IGKN, Wahyuniari IAI, Wiryawan IGNS. Potential of Phytochemical Compounds in Plants in Lowering Blood Glucose Levels in Diabetes Mellitus. *J Science and Health*. 2022;4(5):548-556. doi:10.25026/jsk.v4i5.1259
5. Perkeni. *Guidelines for the Management and Prevention of Type 2 Diabetes Mellitus in Indonesia 2021*. PB Perkeni; 2021.
6. Alqahtani AS, Hidayathulla S, Rehman T, Elgamal AA, Dib RA El, Alajmi MF. A-amylase and Alpha-Glucosidase Enzyme Inhibition and Antioxidant Potential of 3-Oxolupenal and Katononic Acid Isolated from Nuxia oppositifolia. *Biomolecules*. Published online 2019. doi:doi:10.3390/biom10010061
7. Sy SD, Nst MR, Jannah NR. Analysis of Infusion and Ethanol Extract of Tamarindus indica L, Scurrula Sp, Mimosa pudica D of Fresh and Dry as Amylase Enzyme Inhibitor. 2019;17(2):25-31.
8. Mahfur, Walid M. Antidiabetic combination test between durian leather extract and acarbose by combination index control of antidiabetic enzym α-amylase. *Pharm J Indones*. 2019;16(01):85-95.
9. Melinda NA, Kusumo DW, Indah D, Sari K. Antidiabetes activity of some fractions of Azadirachta indica leaves in vitro based on inhibition of α-amylase enzymes. 2023;27(3):82-87. doi:10.20956/mff.v27i3.28301
10. Mutakin, Fauziati R, Fadhilah FN, Zuhrotun A, Amalia R, Hadisaputri YE. Pharmacological Activities of Soursop (Annona muricata Lin.). Published online 2022:1-17. doi:https://doi.org/10.3390/molecules27041201
11. Lienggonegoro LA. Soursop leaf (Annona muricata) and its potential as an anti-cancer. 2022;(May). doi:10.13057/psnmbi/m060128
12. Rasyidah, Hutasuhut MA. Etnobotany study and pharmacological activity of Annona muricata L. leaves extract. *Chlorophyll*. 2019;3(2):10-14.
13. Agu KC, Eluehike N, Ofeimun RO, et al. Possible anti-diabetic potentials of Annona muricata (soursop): inhibition of α-amylase and α-glucosidase activities. *Clin Phytoscience*. Published online 2019. doi:https://doi.org/10.1186/s40816-019-0116-0
14. Kusuma GPOR. Antihyperglycemic Test of Ethanol Extract of Soursop Leaf (Annona muricata L.) on Blood Sugar Levels of Glucose-Induced Male Mice (Mus musculus) Antihyperglycemic Test of Ethanol Extract of Soursop Leaf (Annona muricata L.) on Blood Sugar Levels of Mal. *J Natur Indonesia*. 2021;19(1):1-5.
15. Opara PO, Enemor VHA, Eneh FU, Emengaha FC. Blood Glucose - Lowering Potentials of Annona muricata Leaf Extract in Alloxan - Induced Diabetic Rats. *Eur J Biol Biotechnol*. 2021;2(2):106-113.
16. Ogunyemi OM, Gyebi GA, Saheed A, et al. Inhibition mechanism of alpha-amylase, a diabetic target, by a steroidal pregnane and pregnane glycosides derived from Gongronema latifolium Benth. *Frontiers (Boulder)*. 2022;(August):1-19. doi:10.3389/fmolb.2022.866719
17. Ischak NI, Musa WJA, Aman LO, Alio L, Kilo A La, Saleh SD. Molecular Docking Study and ADME Prediction of Secondary Metabolite Compounds of Gorontalo Traditional Medicinal Plants against HER-2 Receptor as Breast Anticancer. 2023;5(1):90-103.
18. Renadi S, Tri A, Pratita K, Mardianingrum R. The Potency of Alkaloid Derivates as Anti-Breast Cancer Candidates: In Silico Study. 2023;9(May):89-108. doi:10.15408/jkv.v9i1.31481

19. Hanif AU, Lukis PA, Fadlan A. Effect of MMFF94 Energy Minimization with MarvinSketch and Open Babel PyRx on. *Alchemy J Chem*. Published online 2021.
20. Ruswanto R, No T, Mardianingrum R, Kesuma D. Design, molecular docking, and molecular dynamics of thiourea-iron (III) metal complexes as NUDT5 inhibitors for breast cancer treatment. *Heliyon*. 2022;8(April). doi:10.1016/j.heliyon.2022.e10694
21. Umar AB, Uzairu A, Uba S, Shallangwa GA. In silico Studies of some potential anti-cancer agents on M19-MEL cell line. *Moroccan J Chem*. 2021;9(2):260-273.
22. Pan A, Pranavathiyani G, Chakraborty S Sen. Chapter 8 - Computational Modeling of Protein Three-Dimensional Structure: Methods and Resources. In: Coumar MSBTMD for CADD, ed. Academic Press; 2021:155-178. doi:https://doi.org/10.1016/B978-0-12-822312-3.00023-0
23. Noer S, Khairullah MF. In-Silico Study of Luteolin Compound as Breast Anticancer Drug Candidate. *Semin Nas Sains*. 2023;1(1):16-22. https://prediction.charite.de/
24. Komari N, Hadi S, Suhartono E. Protein modeling with Homology Modeling using SWISS-MODEL. *J Network Mat and Science*. 2020;2(2):65-70. doi:10.36873/jjms.2020.v2.i2.408
25. Sumitha A, Devi PB, Hari S, Dhanasekaran R. COVID-19 - In Silico Structure Prediction and Molecular Docking Studies with Doxycycline and Quinine. *Biomed Pharmacol J*. 2020;13(3):1185-1193. doi:10.13005/bpj/1986
26. Gaffar S, Masyhuri AA, Hartati YW, Rustaman R. Studi in Silico Single Chain Variable Fragment (Scfv) Selektif Terhadap Hormon Basic Natriuretic Peptide (Bnp). Chimica et Natura Acta. 2016 Aug 12;4(2):52-9.
27. Ramachandran GN, Ramakrishnan C, Sasisekharan V. Stereochemistry of Polypeptide Chain Configurations. *J Mol Biol*. 1963;7(1):95-99. doi:10.1016/S0022-2836(63)80023-6
28. Ghandadi M. An Immunoinformatic Strategy to Develop New Mycobacterium tuberculosis Multi - epitope Vaccine. *Int J Pept Res Ther*. 2022;28(3):1-14. doi:10.1007/s10989-022-10406-0
29. Oladejo DO, Oduselu GO, Dokunmu TM, et al. In silico Structure Prediction, Molecular Docking, and Dynamic Simulation of Plasmodium falciparum AP2-I Transcription Factor. *J Genet Eng Biotechnol*. 2023;21(44). doi:10.1177/11779322221149616
30. Rastini MBO, Giantari NKM, Andyani KD, Udayana NPL. Molecular Docking Anticancer Activity of Quercetin Against Breast Cancer In Silico. Published online 2019. doi:https://doi.org/10.24843/JCHEM.2019.v13.i02.p09
31. Nuraini M, Ruswanto R. In Silico Study of Galangin Compound of Galangal (Alpinia galanga) as Anticancer against Breast Cancer. Published online 2021.
32. Nugroho AW, Fauzi A. Molecular docking study of acetoxychavicol acetate (ACA) flower solutions on target proteins ER-α, ER-β, and HER-2 as cytotoxic agents. *Pharmaceutics*. 2024;13(3):111-122.
33. Naufa F, Mutiah R, Yen Yen IA. In Silico Study of Potential of Green Tea Catechin Compounds (Camellia sinensis) as SARS CoV-2 Antivirus against Spike Glycoprotein (6LZG) and Main Protease (5R7Y). *J food Pharm Sci*. 2022;10(1):584-596.
34. Sari IW, Junaidin, Pratiwi D. Molecular Docking Study of Flavonoid Compound of Herba Kumis Kucing (Orthisiphon stamineus B.) on Alpha-Glucosidase Receptor as Antidiabetes Type 2. *J Farmagazine*. 2020;7(2):54-60.
35. Nursamsiar N, Awaluddin A, Nur S. In Silico Study of Aglycon Curculigoside A and Its Derivatives as α -Amilase In Silico Study of Aglycon Curculigoside A and Its Derivatives as α -Amilase Inhibitors In Silico Study of Aglycon Curculigoside A and Its Derivatives as α -Amilase Inhibitors. 2020;(December). doi:10.24198/ijpst.v7i1.23062
36. Afliana D, Ariyanti D. Molecular Docking Analysis of Secondary Metabolite Compounds from Trichoderma sp. isolates. Against Cutinase Enzyme Receptor in Fusarium Wilt Disease. *J Life Sci Technol*. 2024;2(2):25-39.
37. Ekawasti F, Sa'diah S, Cahyaningsih U, Dharmayanti NLPI, Subekti DT. Molecular Docking of Red Ginger and Turmeric Compounds on Dense Granules Protein - 1 Toxoplasma gondii with In Silico Method. *J Vet*. 2021;22(36):474-484. doi:10.19087/jveteriner.2021.22.4.474
38. Faqiha AF, Indrawijaya YYA, Suryadinata A, Amiruddin M, Mutiah R. Potential of Nitazoxanide and Arbidol Compounds as SARS-CoV-2 Antivirus against NSP5 (7BQY and 2GZ7) and ACE2 (3D0G and 1R4L) Receptors. 2022;5(March 2024). doi:10.22146/jfps.3393
39. Sharma A, Ahmed SSSJ. Network-Derived Radioresistant Breast Cancer Target with Candidate Inhibitors from Brown Algae: A Sequential Assessment from Target Selection to

Quantum Chemical Calculation. *Mar Drugs*. 2023;21(10).
40. Fischer ALM, Tichy A, Kokot J, et al. The Role of Force Fields and Water Models in Protein Folding and Unfolding Dynamics. *J Chem Theory Comput*. 2024;20(5):2321-2333. doi:10.1021/acs.jctc.3c01106
41. Prasetiawati R, Damayanti A, Suwandi DW. Molecular Dynamics Simulation of Active Compounds of Tangkur Fern Root (Polypodium feei METT) as an Inhibitor of Inducible Nitric Oxide Synthase (iNOS) Enzyme. In: *Proceedings of the National Seminar on Research Dissemination*. Vol 3. ; 2023:390-400.
42. Zubair MS, Maulana S, Mukaddas A. Molecular Inhibition and Molecular Dynamics Simulation of Compounds from the Nigella Genus on the Inhibition of HIV-1 Protease Enzyme Inhibitors Activity.) *J Farm Galen*. 2020;6(1):132-140. doi:10.22487/j24428744.2020.v6.i1.14982
43. Sari BL, Suhendar U, Hamdani R. Implementation and simulation of molecular dynamics of bioactive compounds of Eleutherine sp. as a hepatitis B virus capsid inhibitor. *Farmamedika*. 2023;8(2):103-110.
44. Abdalla M, Ali W, El-arabey AA, Singh K, Jiang X. Molecular dynamic study of SARS-CoV-2 with various S protein mutations and their effect on thermodynamic properties. *Comput Biol Med*. 2021; (November).
45. Gholam GM. Molecular docking of the bioactive compound Ocimum sanctum as an inhibitor of Sap 1 Candida albicans. *Sasambo J Pharm*. 2022;3(1).
46. Moazzam M, Rasheed B, Sarfraz MT, Rana MM, Taj MH. Molecular Interaction Of Acetyl-Coa Carboxylase (Accase) With Fenoxaprop-P Ethyl Through Computational Analysis. *J Pharm Negat Results*. 2023;14(4):554-559. doi:10.47750/pnr.2023.14.04.67
47. Sherlin A, Mathew A, Lakshmipriya M. *Understanding the Activating Mechanism of the Immune System against COVID-19 by Traditional Indian Medicine: Network Pharmacology Approach*. Vol 129. 1st ed. Elsevier Inc; 2022. doi:10.1016/bs.apcsb.2021.11.007
48. Angelina M, Koban G, Lestari SR, Setiowati FK. In Silico Analysis of Naringenin from Stone Root Tubers (Gerrardanthus macrorhizus Harv. ex Benth. & Hook. f.) as Antitussive against N-methyl-D-aspartate Receptor. *J of Life Sciences*. 2022;7(3):172-182. doi:10.24002/biota.v7i3.5912
49. Weni M, Safithri M, Seno DSH. Molecular Docking of Active Compounds Piper crocatum on The Alpha- Glucosidase Enzyme as Antidiabetic Molecular Docking of Active Compounds Red Betel Leaf (Piper Crocatum) on the Alfa-Glucosidase Enzyme as Antidiabetic. *Indones J Pharm Sci Technol*. 2020;7(2):64-72.
50. Karim BK, Tsamarah DF, Zahira A, et al. In-Silico Study of Active Compounds in Guava Leaves (Psidium guajava L.) as Candidates for Breast Anticancer Drugs In-Silico Study of Active Compounds in Guava Leaves (Psidium guajava L.) as. *Indones J Biol Pharm*. 2024;3(3):194-209.
51. Wulandari RP, Gabriel K, Nurdin HA, et al. Indonesian Journal of In Silico Study of Secondary Metabolite Compounds in Parsley (Petroselinum crispum) as a Drug Therapy for Blood Cancer (Myeloproliferative Neoplasm (MPN)) targeting JAK-2. *Chem Sci*. 2023;12(2).
52. Herdini, Setyawati IR. In Silico Study: Active Compounds of Senggugu Root (Clerodendrum serratum) against Human Chitotriosidase-1 (hCHIT1) Receptor Inhibition as Asthma. *SCIENCESTECH*. 2023;33(2):91-107.
53. Ruswanto R, Mardianingrum R, Yanuar A. Computational Studies of Thiourea Derivatives as Anticancer Candidates through Inhibition of Sirtuin-1 (SIRT1). *J Kim Sains dan Apl Vol 25, No 3 Vol 25 Issue 3 Year 2022*. Published online 2022. doi:10.14710/jksa.25.3.87-96
54. Nursanti O. Toxicity prediction and pharmacokinetics to get antidiabetes medicine identification. *J Pharm Care Sci*. 2023;3(2):1-9.
55. Du B xue, Xu Y, Yiu SM, Yu H, Sh JY. ADMET property prediction via multi-task graph learning under adaptive auxiliary task selection. *iScience*. 2023;26. doi:10.1016/j.isci.2023.108285
56. Klimoszek D, Jele M, Dołowy M. Study of the Lipophilicity and ADMET Parameters of New Anticancer Diquinothiazines with Pharmacophore Substituents. *Pharmaceuticals*. 2024;17(6).
57. Effendi N, Saputri NA, Purnomo H, Aminah. In Silico ADME-T and Molecular Docking of Tamoxifen Analogs as Breast Cancer Therapy Agent Candidates. *Media Farm*. 2023;19(1). doi: 10.32382/mf.v19i1.3305

APPENDIX

SUPPLEMANTARY

Table S1. Receptor validation results.

Grid Center Dimension			*Grid Box*			*Spacing*	*RMSD*	*Binding Affinity*	*Run*
X	Y	Z	X	Y	Z	**(Å)**	**(Å)**	*(kcal/mol)*	
2.692	40.975	24.196	40			0.375	0.62 Å	-3,83	80

Table S2. RMSD values of test and comparator compounds.

Compound	Average (Å)	Minimum value (Å)	Max value (Å)
GLC-AGL	2.125	1.082	2.868
Acarbose	2.131	1.070	2.639
Coclaurine	2.005	0.989	2.264
Xylopin	2.005	0.989	2.264
Annomuricine	1.723	1.059	1.968

Table S3. The RMSF values of compounds.

Compound	Minimum Value		Maximum Value	
	RMSF Å	Residue	RMSF Å	Residue
Coclaurine	0.345	Arg195	4.541	Asn350
Xylopine	0.345	Arg195	4.541	Asn350
Annomuricine	0.382	Arg195	4.005	Asn364
Acarbose	0.412	Met338	7.021	Gly351
GLC-AGL	0.443	Asn46	4.623	Tyr2

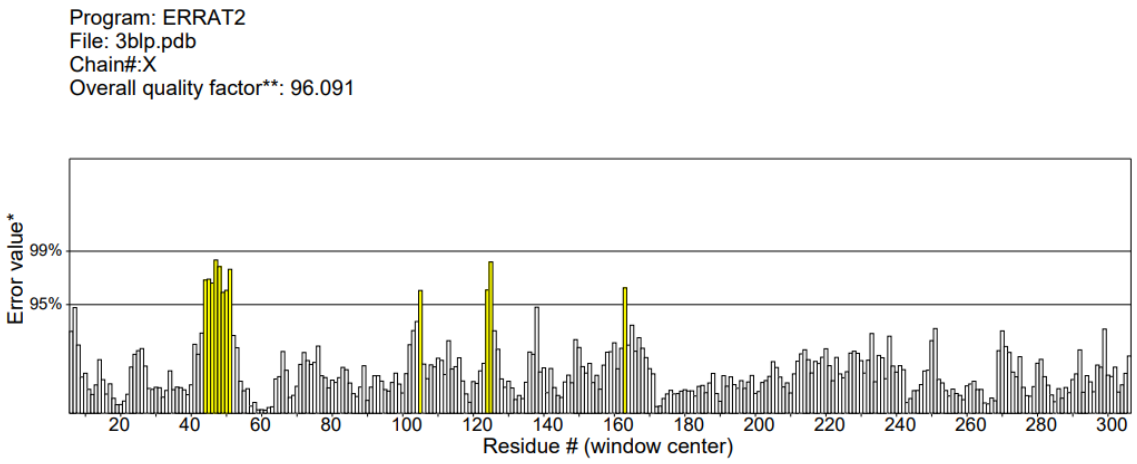

Figure S1. The ERRAT analysis result of enzyme *α-Amylase* (3BLP.pdb).

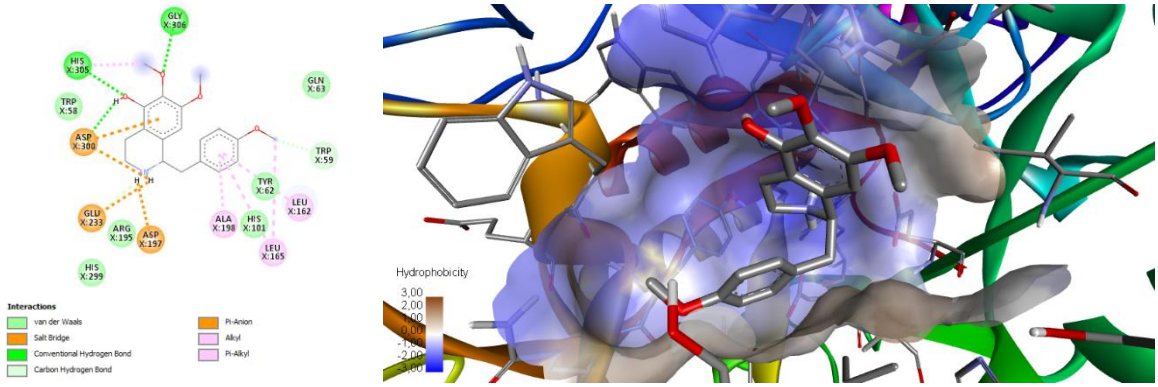

(a)

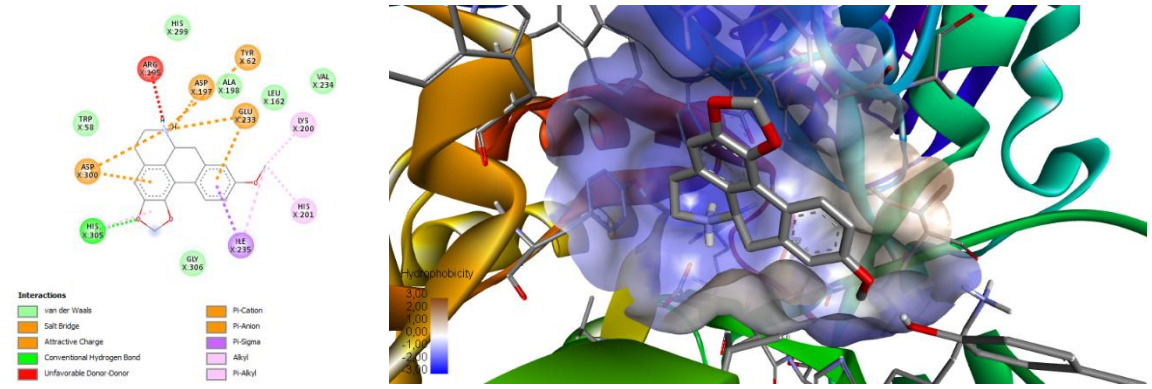

(b)

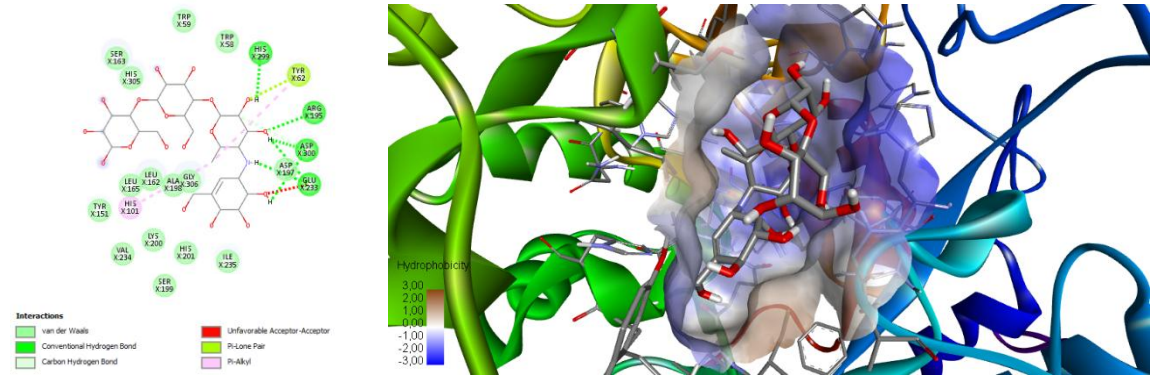

(c)

Figure S2. The 2D/3D Visualization of *α-Amylase* and Xylopine (a); *α-Amylase* and Annomuricine (b, and *α-Amylase* and *Acarbose* (c).

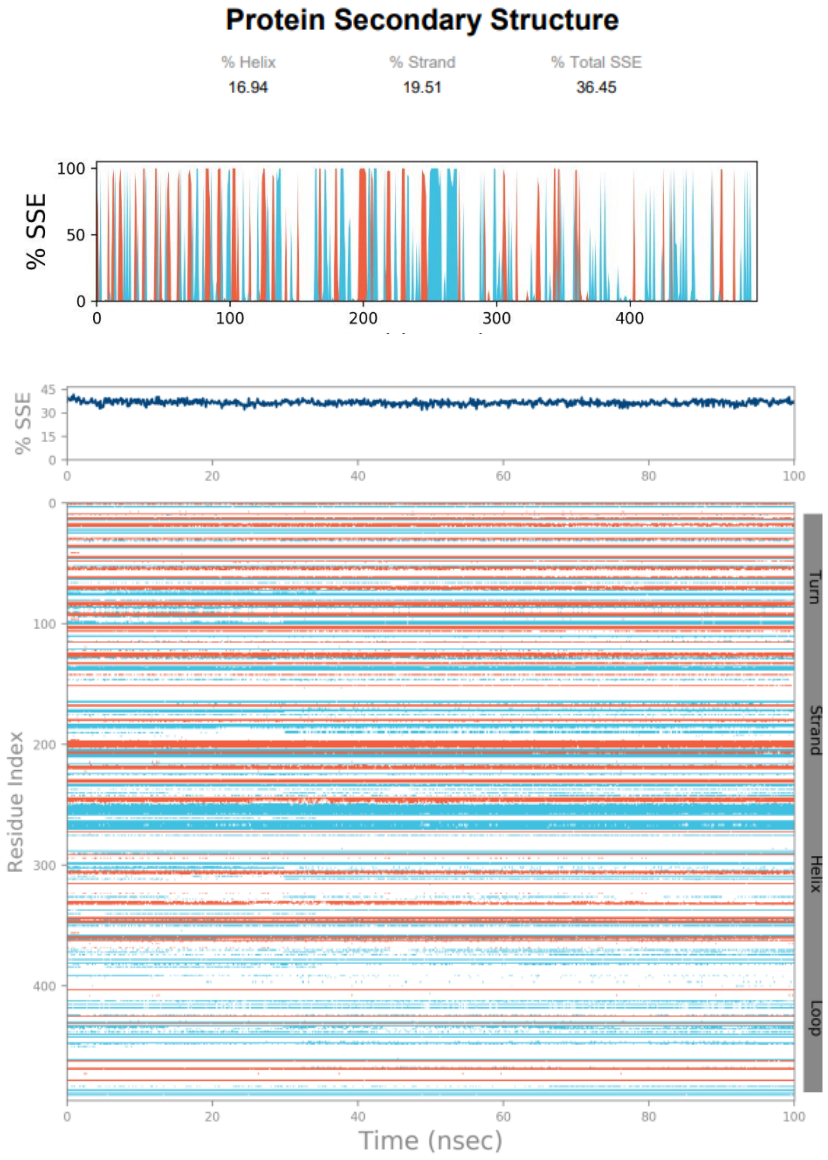

Figure S3. The changed pf protein secondary structure of *α-Amylase* enzyme in molecular Dynamic 100ns.

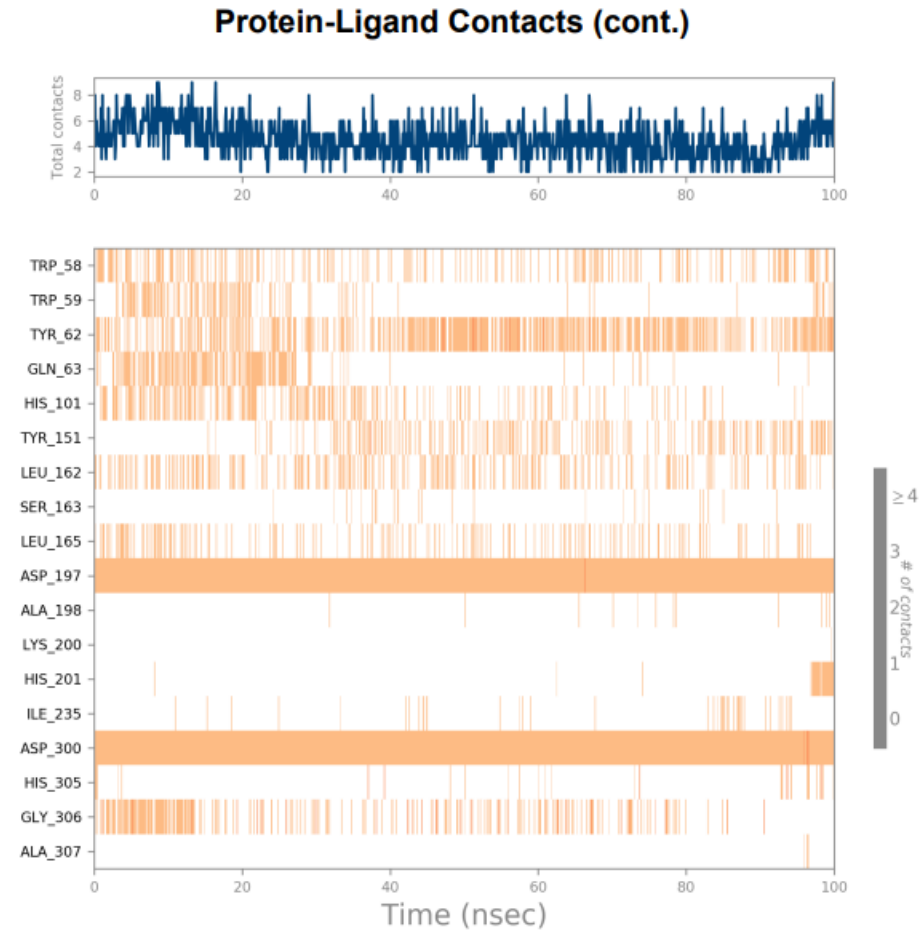

Figure S4. Timeline representation of residual contact of Annomuricine-enzyme α-amylase complex in 100 ns MD. simulation

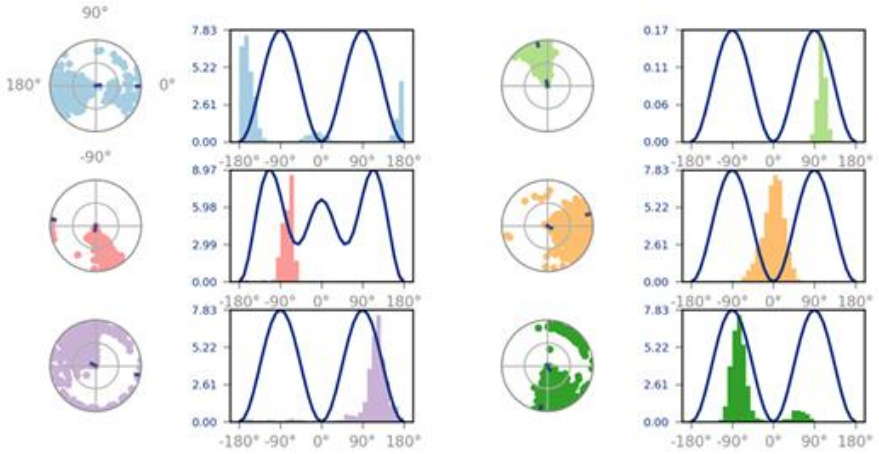

Figure S5. Ligand Torsion Profile of Annomuricine Complex and enzyme α-amylase in 100ns MD simulations.